MINISTRY OF TECHNOLOGY

AERONAUTICAL RESEARCH COUNCIL

REPORTS AND MEMORANDA

Flight Measurements of the Elevator and Aileron Hinge-Moment Derivatives of the Fairey Delta 2 Aircraft up to a Mach Number of 1·6 and Comparisons with Wind-tunnel Results

By R. Rose, M.Sc., O. P. Nicholas, B.Sc.(Eng.) and Glynis Vorley

LONDON: HER MAJESTY'S STATIONERY OFFICE

1967

PRICE 15s. 6d. NET

Flight Measurements of the Elevator and Aileron Hinge-Moment Derivatives of the Fairey Delta 2 Aircraft up to a Mach Number of 1·6 and Comparisons with Wind-tunnel Results

By R. Rose, M.Sc., O. P. Nicholas, B.Sc.(Eng.) and
Glynis Vorley

Summary.

Aileron and elevator hinge-moment derivatives have been extracted from flight tests on the Fairey Delta 2 in which the dynamic aircraft response. to control pulses was recorded. As this method is not widely used, and has proved very successful, it is described in detail. Corrections had to be made for aeroelastic distortion of the control surfaces, for inertia loads acting on the controls and for the dynamic response of the instrumentation.

Where possible the results are compared with wind-tunnel data. There is good agreement for the hinge moment due to control derivatives, b_2, and the elevator, b_1, whereas the results for aileron, b_1, show differences from the tunnel values at supersonic speeds.

b_0 could not be measured because of strain gauge drift; however consistent results were obtained for the aileron hinge moment induced by the elevator deflection and *vice versa*. At transonic speeds these terms are of similar magnitude to the conventional hinge moment derivatives b_1 and b_2, and must therefore be considered by designers.

LIST OF CONTENTS

1. *Introduction.*

There is considerable interest in predicting values of the hinge moments for controls. At present there are no reliable theories[1] for estimating hinge moments at transonic and supersonic speeds, and predictions, for these cases, are usually based on wind-tunnel results. To give confidence in these predictions, it is important that some checks are made between tunnel and flight measurements. This report presents the results of flight measurements made at R.A.E. Bedford, of trailing edge control hinge moments on the Fairey Delta 2, which is a research aircraft with a control configuration of current interest and a performance well into the supersonic speed range. The flight results are compared with tunnels results[2,3] made at transonic and supersonic speeds.

A dynamic flight test technique has been used, which allows the elevator and aileron hinge-moment derivatives, with the exception of b_0, the hinge moment at zero incidence and control angle, to be extracted.

2. *Description of Aircraft and Instrumentation.*

2.1. *Aircraft.*

The Fairey Delta 2 is a 60 deg delta wing tailless research aircraft capable of speeds up to at least $M = 1.7$. Fig. 1 shows a general arrangement and Fig. 2 a photograph of the aircraft. Table 1 gives the principal dimensions of the aircraft and Table 2 details of the control surfaces.

The aircraft has full-span trailing-edge controls, which are split into separate elevators and ailerons; the elevators are aerodynamically unbalanced, the ailerons are rigged up 3 deg and have a small horn balance. The control surfaces are operated by irreversible hydraulic jacks. The elevator jacks are positioned in the rear fuselage and operate the elevators *via* torque tubes. The aileron jacks are situated beneath the outer wing, forward of the mid portion of the aileron, and operate the ailerons directly.

Control-feel forces are supplied to the pilot by simple springs, the datum of each spring being varied, within a limited range, by an electric trim motor. To cater for the large variations of aircraft response and control effectiveness over the flight envelope, the gear ratios between the elevators and ailerons and the corresponding stick movement, can be varied in flight by the pilot.

2.

2.2. *Instrumentation.*

The following parameters, relevant to the tests, were recorded on Hussenot A.22 photographic trace recorders:

Speed
Altitude
Elevator angle (port and starboard)
Aileron angle (port and starboard)
Elevator hinge moment (port and starboard)
Aileron hinge moment (port and starboard)
Strain-gauge bridge voltage
Incidence
Normal acceleration
Rate of roll
Sideslip angle

The hinge moments were measured with four-active-arm strain-gauge bridges energised by a stabilised voltage from Venner accumulators. In the case of the elevators the strain gauges were attached to the inner surface of the torque tubes; for the ailerons the gauges were attached to one end of the jack body. A typical strain increment in the tests was 0·02 per cent. The strain gauges were carefully matched and during ground tests were found to have negligible drift over a temperature range −40 deg C to +40 deg C. The bridges have been calibrated by applying known loads to the control surfaces. Control-surface angles were measured by potentiometers attached to the controls.

Incidence was measured by one of four wind vanes mounted on the nose boom of the aircraft behind the pitot-static head. The vanes were arranged in a cruciform configuration so as to preserve the symmetrical arrangement required to reduce position errors in the transonic and supersonic speed range.

3. *Flight Tests.*

The main flight tests consisted of recording the control hinge moments and the response of the aircraft during and after either an elevator or aileron pulse. Due to the lack of control of thrust with reheat on and the limited fuel available, it was not possible in this aircraft at transonic and supersonic Mach numbers to stabilise speed. This caused some difficulty in trimming the aircraft, particularly at transonic speeds where significant trim changes occurred rapidly. Nevertheless, pilots found it possible, after some practice, to trim the aircraft satisfactorily during these non-stabilised conditions. With the aircraft in trim, the pilot tapped the control column in either a lateral or rearwards direction and allowed it to return to its trim position under the action of the feel spring, resulting in a control pulse of about one quarter second duration*. This was the shortest pulse possible, and gave a good compromise between the requirements that the aircraft should not have responded significantly by the time the peak of the pulse had been reached, and that unsteady aerodynamic effects should be negligible (Appendix A). In some cases a combination of elevator and aileron movement occurred due to the difficulty of moving the control column precisely in the desired direction. For the elevator tests, both the initial response during the pulse and the ensuing longitudinal short-period oscillation of the aircraft were used in the analysis. However, for the aileron pulses, only the initial response has been analysed, as the hinge moments induced by the dutch roll oscillation were too small to measure accurately. At 40 000 ft, control pulses were recorded in level flight at Mach numbers from 0·86 to 1·6, further tests were made in level flight at 10 000 ft, at Mach numbers from 0·6 to 1·2.

Some supplementary tests were made, in which records were taken during level flight and turns at constant normal acceleration. These tests covered a range of Mach numbers from 0·85 to 1·07 at 40 000 ft and from 0·55 to 0·97 at 10 000 ft.

---

*For a fully irreversible system no further movement should occur. However, the hydraulic jacks did allow some small residual movement of the control surface.

4. *Method of Analysis.*

The incidence vane readings have been corrected for the effects of boom interference evaluated by wind-tunnel calibrations[4], and, in addition at subsonic speeds, for estimated wing and body upwash. Calculation showed that the effect of pitching velocity on the vane readings was negligible, and this was therefore ignored.

The control surfaces are subject to aeroelastic distortion, especially at high speed. Flight pressure-plotting tests made earlier have shown that the aerodynamic loading is reasonably uniform, and making this assumption, the mean angular distortion of the control is directly related to the jack load. In ground tests[5] the distortion of the controls was measured under uniform loading conditions. This distortion was measured relative to the jack output point since the control surface transmitters were attached at this position. The effective stiffnesses of the elevator and aileron are respectively two thousand lb ft/degree and about forty thousand lb ft/degree. Two factors contribute to this large difference in stiffness. Firstly, the jack load is applied near the aileron mid-span, whereas it is applied at the root-end of the elevator. Secondly, in the case of the elevator, flexibility of the linkage between the jack output and elevator root accounts for about two-thirds of the measured distortion. In the present flight tests, it has been calculated that significant elevator distortion occurred and this has been allowed for, but that the aileron distortions were negligible.

Appendix A derives the relations between the measured control jack loads and the aerodynamic and inertia loadings on the controls. The jack loads were measured by strain gauges, and although these were carefully matched some drift occurred due to differential-temperature effects. Thus it has not been possible to determine absolute values of jack loads very accurately, but as the rate of drift was sufficiently slow in relation to the duration of most of the manoeuvres executed during the tests, incremental values of the jack moments could be measured with confidence.

The dynamic response of the recording galvanometers and ratiometers has been allowed for in the analysis. Simple laboratory checks showed that amplitude ratio effects were just significant in some cases.

A number of assumptions have been made in the analysis of the flight results and these are listed below.

(a) All hinge-moment derivatives are linear within the range covered during each individual test, but they are not necessarily linear over the full range of control angles and incidences covered in the flight tests.

(b) The shape of a control pulse may be represented by the first half of a sine wave.

(c) The change in aircraft incidence, up to the instant where an elevator pulse has its maximum, is small.

(d) The changes in sideslip and rate of roll, up to the instant where an aileron pulse has its maximum, are small.

(e) Movement of the controls is small, but possibly significant, during the aircraft oscillations following an elevator pulse.

(f) The distorted elevator can be represented by an undistorted control at an appropriate mean angle.

(g) In applying the distortion corrections the aerodynamic and inertia loadings are assumed uniform over the control surface.

(h) Calibrations of the control jack load and the surface distortions may be extrapolated linearly to the considerably higher flight loading conditions.

4.1. *Elevator Pulses.*

Fig. 3a illustrates an idealised elevator pulse test, showing time histories of the elevator and aileron jack moments, and incidence, during and following the pulse. A corresponding actual flight record is shown for comparison, Fig. 3b. The essential differences between the actual and idealised records are that, in practice, a small, but negligible, change of incidence occurs before the peak of the pulse, and also the elevator does not return precisely to its trimmed value at the cessation of the pulse. However, these effects are quite small and thus it is possible to use simple methods of analysis. This analysis is conveniently split into two parts, treating first the response during the pulse and then the ensuing aircraft oscillation.

4

From the increments in the control jack loads and the elevator angle between the trimmed conditions and values at the peak of the elevator pulse, according to equations B.7 and B.8 of Appendix B, the hinge moment derivatives b_{2_E} and $\partial C_{H_A}/\partial \eta$ may be derived. b_{2_E} is the elevator hinge moment due to elevator angle derivative, and $\partial C_{H_A}/\partial \eta$ is the aileron hinge moment due to elevator angle derivative. This latter derivative is not normally considered, but it was found in these tests to be of a very considerable magnitude. The inertia term, in equations B.7 and B.8, amounts typically to 5 per cent of the total measured hinge moment.

The elevator pulse excites the longitudinal short period oscillation of the aircraft. Appendix C, equations C.4 and C.5, shows how measurements made during the oscillation allow b_{1_E} and b_{1_A} to be determined. b_{1_E} is the elevator hinge moment due to incidence derivative, and b_{1_A} is the aileron hinge moment due to incidence derivative. In this case the inertia term amounts typically to 15 per cent of the measured total hinge moment. The analysis uses values of the recorded quantities only at the peaks of the oscillation. In practice it was found that reliable results could be obtained at supersonic speeds; however, at subsonic speeds, due to increased residual control motion following the pulse, and increased damping of the air-craft oscillation, the method could only be applied in some cases. In this regime an alternative technique was required to obtain measurements of b_{1_E} and b_{1_A}, and this is discussed in Section 4.3.

4.2. *Aileron pulses.*

Figs. 4a and b show idealised and actual flight records of an aileron pulse. The initial response of the aircraft is a rapid acceleration in roll with practically no change in sideslip and rate of roll. The aileron and elevator hinge moments closely follow the aileron angle input.

Equations B.10 and B.11, of Appendix B, show how b_{2_A} and $\partial C_{H_E}/\partial \xi$ can be obtained from measurements of incremental control loads and the aileron angle between the trimmed conditions and the peak of the pulse. b_{2_A} is the aileron hinge moment due to aileron-angle derivative, and $\partial C_{H_E}/\partial \xi$ is the elevator hinge moment due to aileron-angle derivative. The latter derivative represents the effect on the elevator hinge moment of aileron angle deflection, which was found to be considerable in the present tests. The inertia terms in these cases amount typically to 15 per cent of the total hinge moment.

4.3. *Steady Turns.*

At subsonic speeds the damping of the longitudinal short period oscillation of the aircraft is high, and as mentioned earlier, under these conditions it is not possible to extract b_{1_E} and b_{1_A} from elevator pulse tests. However, by measuring the elevator and aileron jack loads in steady flight at the same Mach number but at two different values of normal acceleration, it is possible to evaluate b_{1_E} and b_{1_A} as shown in Appendix D. The required tests were made by accelerating the aircraft in level flight through the desired range of Mach number, and then decelerating the aircraft in a steady turn. By comparing values recorded at the same Mach number during the two parts of such a flight test, the data required for analysis are obtained. It should be noted that in this case absolute rather than incremental jack loads are required, and as an appreciable time interval is involved between the recording of corresponding test points, strain gauge drift may become significant, and as a consequence the accuracy is reduced. Also any two flight points used in this analysis differ not only in incidence, but also in the elevator and aileron angles required to trim. The contributions due to control movement terms are generally larger than those due to b_{1_E} and b_{1_A} which are to be extracted from the tests. As a consequence the accuracy of the final result is further reduced.

5. *Results and Discussion.*

Fig. 5, 6 and 7 show the ranges of aileron angle, elevator angle and incidence explored during the tests. These envelopes are presented because tunnel tests show that, in some cases, hinge moments vary non-linearly with incidence and control angle; thus values of derivatives depend on the range of control angle and incidence used in a particular test. As an example, Fig. 8 shows some tunnel measurements of aileron hinge moment at $M = 1.02$, and the range of elevator angle and incidence covered in the flight tests at 10 000 ft and 40 000 ft. It can be seen that b_{1_A} and $\partial C_{H_A}/\partial \eta$ would be expected to differ at the two altitudes.

Figs. 9 to 14 show the variation with Mach number of the measured values of b_{1_E}, b_{2_E}, $\partial C_{H_E}/\partial\xi$, b_{1_A}, b_{2_A} and $\partial C_{H_A}/\partial\eta$. The flight results include data from tests at 10 000 ft and 40 000 ft using both pulse and steady turn techniques. Where possible comparable wind tunnel data[2,3] are also shown. In the cases where the tunnel tests showed non-linear variations with incidence and control angle, the derivatives were extracted by considering the incidence and control angle appropriate to the corresponding flight conditions (Fig. 8).

The flight values of the elevator hinge moment due to incidence derivative b_{1_E}, Fig. 9, show some scatter, particularly at transonic speeds where as noted in Section 4.3 the accuracy of the analysis is particularly poor, but the variation with Mach number is well defined. b_{1_E} shows a rapid increase at transonic speeds and a gradual decrease at supersonic speeds. There is no detectable difference between the results at 10 000 ft and 40 000 ft, and this suggests that the fairly simple method used to correct the results for the aeroelastic distortion of the elevator has been adequate, and confirms the tunnel results which show no non-linearities over the range of elevator angle and incidence explored. The comparison with wind-tunnel results is good.

For the elevator hinge moment due to elevator-angle derivative b_{2_E}, Fig. 10, the same general remarks as made for b_{1_E} apply. b_{2_E} is roughly twice as large as b_{1_E}.

Fig. 11 shows the variation of the elevator hinge moment due to aileron-angle derivative, $\partial C_{H_E}/\partial\xi$, with Mach number. The results show very little scatter, and the derivative is well defined. $\partial C_{H_E}/\partial\xi$ is small at subsonic and supersonic speeds, but increases rapidly at transonic speeds. This derivative has normally been ignored by designers, but clearly its effect on the control hinge moments of this configuration at transonic speeds is very significant. The wind-tunnel tests do not provide data on this derivative.

The flight results for the aileron hinge moment due to incidence derivative b_{1_A} are shown in Fig. 12. In the subsonic range results from the two alternate test procedures are shown. They differ quite significantly. From the previous discussions on the steady turn tests, it would appear that these are generally less reliable, and as a consequence more weight has been given when drawing a mean line through the test points to the results of the pulse tests. There is a rapid increase in b_{1_A} at transonic speeds followed by a rapid decrease at supersonic speeds. No aeroelastic corrections have been applied since the calculated distortion of the ailerons was negligible. However, there are quite significant differences between the results obtained at 10 000 ft and 40 000 ft. These differences could be due to either an aeroelastic distortion of the wing, or a non-linear variation of hinge moment over the different ranges of elevator angle and incidence appropriate to the two test heights. At transonic speeds wind-tunnel results[2,3] show marked non-linear variations of hinge moment with incidence and elevator angle, for example as shown in Fig. 8. At supersonic speeds wind-tunnel values of the derivative extracted for the 40 000 ft flight conditions are considerably higher than the corresponding flight measurements. No corresponding wind-tunnel data are available for the 10 000 ft flight conditions as the appropriate ranges of aircraft parameters were not covered in the tunnel programme. However, extrapolation of tunnel data in the range $M = 1\cdot1$ to $1\cdot2$, suggests that b_{1_A} at conditions appropriate to flight at 10 000 ft is approximately 0·6 less than at 40 000 ft. This difference is almost identical to that between flight results at the two test altitudes. This suggests that the apparent effects of altitude in the flight results shown in Fig. 12 are mainly due to non-linearities in the hinge moment characteristics.

The results for the aileron hinge moment due to aileron-angle derivative b_{2_A}, Fig. 13, show very little scatter. The results at 10 000 ft and 40 000 ft are different. Again it is thought that this is probably caused by non-linear effects, but no wind-tunnel results are available for comparison.

Fig. 14 shows the variation of the aileron hinge moment due to elevator derivative, $\partial C_{H_A}/\partial\eta$, with Mach number. This derivative has been generally ignored in the past; however, in this configuration, although it is small at subsonic and supersonic speeds, it is significant at transonic speeds and is indeed then of the same magnitude as b_{2_A}. Wind-tunnel results show a transonic peak in good agreement with the flight measurements, but at supersonic speeds, whereas the variation is similar, the agreement is not so good. The effect of the inter-control gap on $\partial C_{H_A}/\partial\eta$ must be considerable, hence it is possible that Reynolds number effects may be causing this discrepancy. The present tests have shown that at transonic speeds the influence of one trailing edge control on the hinge moment of an adjacent control is considerable.

6. *Conclusions.*

The elevator and aileron hinge-moment derivatives of the Fairey Delta 2 have been determined, using dynamic techniques, up to Mach numbers of 1·2 and 1·6 at 10 000 ft and 40 000 ft respectively. Where possible, comparison has been made with wind-tunnel results[2,3] obtained with a 1/9th scale model. The results are summarised in Figs. 8 to 13.

All the derivatives show a characteristic rapid increase at transonic speeds followed by a reduction at supersonic speeds. For the elevator, it has been necessary to correct for the aeroelastic distortion of the control; a relatively simple method of analysis has been used with success, and the results of tests at 10 000 ft and 40 000 ft agree well with one another. On the basis of ground tests, it was calculated that no significant aeroelastic distortion of the ailerons occurred. In this case, the 10 000 ft and 40 000 ft results show considerable differences; wind-tunnel tests suggest this is probably due to non-linearity of the hinge-moment characteristics over the range of elevator angle and incidence appropriate to the two test heights. The results show that at transonic speeds the influence of one trailing-edge control on the hinge moment of an adjacent control can be considerable. The influence of this derivative on control hinge moments has normally been ignored by designers in the past; it would appear that this effect should be taken into account in appropriate cases.

Although some of the flight results show considerable scatter, the derivatives are reasonably well defined and the agreement with wind-tunnel results is reasonable in view of the difficulties involved in the test techniques and the non-linear variation of some of the derivatives.

LIST OF SYMBOLS

A	Aircraft rolling moment of inertia	slugs/ft^2
$a = \dfrac{\partial C_L}{\partial \alpha}$	Lift-curve slope	
B	Aircraft pitching-moment inertia	slugs/ft^2
b_{0_E}	Constant in equation (A.2)	
$b_1 = \dfrac{\partial C_H}{\partial \alpha}$		
$b_{2_A} = \dfrac{\partial C_{H_A}}{\partial \xi}$		
$b_{2_E} = \dfrac{\partial C_{H_E}}{\partial \eta}$		
c	Mean chord of control, aft of the hinge line	ft
$\bar{c}$	Wing mean aerodynamic chord	
$C_{H_A} = \dfrac{H_A}{\frac{1}{2}\rho_0 V_i^2 S_A c_A}$	Aileron hinge-moment coefficient	
$C_{H_E} = \dfrac{H_E}{\frac{1}{2}\rho_0 V_i^2 S_E c_E}$	Elevator hinge-moment coefficient	
C_L	Lift coefficient	
$g = 32 \cdot 18$		ft/sec^2
H	Aerodynamic hinge moment of a control, nose up positive	lb/ft
H_J	Elevator jack moment, nose up positive	lb/ft
H_k	Aileron jack moment, nose up positive	lb/ft
$i_A = \dfrac{A}{m s^2}$		
$i_B = \dfrac{B}{m \bar{c}^2}$		
I	Moment of inertia of a control about the hinge line	slugs/ft^2
$\mathscr{J}$	Circular frequency of the aircraft longitudinal short-period oscillation	sec^{-1}
l_ξ	Aileron rolling power	
m_A	Aileron mass	slugs
m_E	Elevator mass	slugs
m	Aircraft mass	slugs
n	Normal acceleration	'g' units
p	Aircraft rate of roll, positive to starboard	rad/sec

q	Aircraft rate of pitch, positive nose up	rad/sec
$(\bar{q}/\bar{n})$	Amplitude ratio of rate of pitch to normal acceleration in the longitudinal short period oscillation	
r_A	*See* Fig. 15	ft
r_E	*See* Fig. 15	ft
S_A	Aileron area, aft of hinge	ft²
S_E	Elevator area, aft of hinge	ft²
S	Wing area	ft²
s	Wing semispan	ft
T	Duration of control pulse	sec
V	true airspeed	ft/sec
V_i	Equivalent airspeed	ft/sec
x_A	*See* Fig. 15	ft
x_E	*See* Fig. 15	ft
y_A	*See* Fig. 15	ft
y_E	*See* Fig. 15	ft
α	Aircraft incidence	radians
$\partial C_m/\partial \eta$	Elevator pitching power	
Δ	Incremental values of parameters	
λ	Sweep of control hinge line	degrees
η	Elevator angle, trailing edge down positive, measured in a plane parallel to the aircraft centreline	radians
ξ	Aileron angle, trailing edge of either surface down positive, measured in a plane parallel to the aircraft centreline	radians
$\rho_0 \quad = 0.002378$	Air density at sea level	slugs/ft³

NOTE: A dot above any of the above quantities denotes differentiation with respect to time.

Suffices

A	Aileron
E	Elevator
1 $\Big\}$	Conditions in steady turns at different normal accelerations
2	

9

REFERENCES

No.	Author(s)	Title, etc.
1	W. E. A. Acum	The comparison of theory and experiment for oscillating wings. A.R.C. C.P.681. March 1962.
2	P. G. Hutton and D. Morton	Results of pressure plotting and control hinge moment tests on a 1/9 scale model of Fairey Delta 2 in the A.R.A. transonic tunnel. A.R.A. Model test note J12/1.
3	G. F. Moss and R. W. Hayward	Unpublished M.O.A. Report.
4	F. W. Dee and D. G. Mabey	Wind tunnel calibrations of incidence vanes for use on the Fairey ER 103. *Jl. R. aeronaut. Soc.* Vol. 67, No. 628, p. 267. April 1963.
5	R. Rose, A. A. Woodfield and C. S. Barnes	Flight measurements of the lift, longitudinal trim and drag of the Fairey Delta 2 at Mach numbers up to 1·65 and comparisons with wind-tunnel results. R.A.E. T.R. 67036. June 1967.
6	M. Shinbrot	On the analysis of linear and non-linear dynamical systems from transient-response data. NACA TN 3288. December 1954.
7	W. E. A. Acum	Aerodynamic forces on a rectangular wing oscillating in a supersonic air stream. R. & M. 2763, A.R.C. August 1950.
8	F. W. Dee	Flight measurements at subsonic speeds of the aileron rolling power and lateral stability derivatives l_v and y_v on a 60 deg delta wing aircraft (Fairey Delta 2). A.R.C. C.P. 739. June 1963.
9	M. D. Dobson	Wind tunnel tests at supersonic speeds of the Fairey Delta 2. A.R.C. C.P. 672. October 1962.
10	D. J. Kettle	8 ft × 6 ft transonic wind tunnel tests on a 1/24 scale model of the Fairey Delta 2 (ER 103). A.R.C. C.P. 656. May 1962.
11	S. Neumark	Analysis of short-period longitudinal oscillations of an aircraft: interpretation of flight tests. A.R.C. R. & M. 2940. September 1952.
12	D. R. Andrews	Measurements in flight of the longitudinal stability derivatives of a 60 deg delta wing aircraft (Fairey Delta 2). A.R.C. C.P. 639. April 1959.

APPENDIX A

The Hinge Moments Acting on Elevator and Aileron Controls.

Fig. 15 shows the relevant geometric data for the control configuration under discussion. The hinge line of both surfaces is swept, and this introduces certain difficulties in the definition of the various quantities involved. Unfortunately there is no clearly established rule to guide us here, and it is therefore proposed to use the following definitions which have also been adopted for the Royal Aeronautical Society aerodynamic data sheets. Control angles and chords are measured in a plane parallel to the plane of symmetry of the aircraft, whilst the hinge moments are measured about the swept control hinge line.

A further difficulty arises as the conventional definition for positive aileron deflection is trailing edge down for the starboard aileron and trailing edge up for the port surface, whereas trailing edge down is normally considered positive in hinge moment notation; the latter definition is used here.

At any instant in flight the sum of the control jack moment, the aerodynamic hinge moment and the inertia reactions is zero. Using the definitions shown in Fig. 15, it can be shown for the starboard elevator that the control jack moment is given by:

$$-H_J = H_E + r_E\, m_E\, gn - (x_E\, r_E\, m_E + I_E \cos \lambda)\dot{q} - I_E \sec \lambda\, \ddot{\eta} - (y_E\, r_E\, m_E - I_E \sin \lambda)\dot{p} \tag{A.1}$$

where the small term due to the aircraft acceleration along the flight path has been ignored. H_J is the jack moment, H_E is the aerodynamic hinge moment, both measured trailing edge down positive, and I_E the control inertia about the hinge axis. Similar equations may be written for the other three control surfaces.

The aerodynamic hinge moment is a function of control deflection and the aerodynamic quantities describing the aircraft motion, these relationships not always being linear. In theory such a situation can be dealt with by an 'equations of motion' technique such as that proposed for the extraction of aircraft stability derivatives by Shinbrot[6], but this would require a resolution of the test data well beyond the accuracy available from the present flight tests. As the control pulses and consequent aircraft responses used during the flight tests were generally rather small, it was assumed that the hinge-moment characteristics could be linearised for the range of parameters covered in each test, and the formal analysis has been made using linearised equations.

Consequently for the elevator, H_E is expanded as

$$H_E = \tfrac{1}{2}\rho_0\, V_i^2\, S_E\, c_E \left[b_{0_E} + b_{1_E}\alpha + b_{2_E}\eta + \frac{\partial C_{H_E}}{\partial \xi}\xi + \frac{\partial C_{H_E}}{\partial \left(\dfrac{q\, c_E}{V}\right)} \frac{q c_E}{V} + \right.$$
$$\left. + \frac{\partial C_{H_E}}{\partial \left(\dfrac{\dot{\eta}\, c_E}{V}\right)} \frac{\dot{\eta} c_E}{V} + \frac{\partial C_{H_E}}{\partial \left(\dfrac{\dot{\alpha}\, c_E}{V}\right)} \frac{\dot{\alpha} c_E}{V} \right]. \tag{A.2}$$

The term $\partial C_{H_E}/\partial \xi$ represents the elevator hinge moment induced by aileron deflection; in the present tests this term was found to be comparable in magnitude with primary control derivatives b_{1_E} and b_{2_E}.

As the strain gauges used to measure the jack moments were unable to give reliable absolute values, almost all the analysis was made using incremental values. As a consequence b_0 could not be determined.

The frequency and amplitude of the control movements used were considerably larger than those of the resulting aircraft motion and thus one would expect any unsteady aerodynamic effects to be more important for the former. Estimates based on Acum[1,7] suggest that at supersonic speeds unsteady contributions are very small compared with those from the steady aerodynamic effects; while at the subsonic speeds tested they might produce up to 2 per cent change in the peak hinge moment, and a phase displacement of 12 deg between the peaks of the control input and resulting hinge moment. In fact, the flight

11

records showed that the peak of the hinge moment did not lag by more than 10 deg behind the peak of the control input. Since this is equivalent to less than 2 per cent in amplitude, it has been assumed that unsteady effects have a negligible influence on the level of the hinge moment peaks.

Thus equation (A.2) is reduced to

$$\Delta H_E = \tfrac{1}{2}\rho_0 V_i^2 S_E c_E \left(b_{1_E} \Delta\alpha + b_{2_E} \Delta\eta + \frac{\partial C_{H_E}}{\partial\xi} \Delta\xi \right) \tag{A.3}$$

where the symbol Δ denotes incremental values.

For the starboard elevator equations (A.1) and (A.3) give

$$-\Delta H_J = \tfrac{1}{2}\rho_0 V_i^2 S_E c_E \left(b_{1_E} \Delta\alpha + b_{2_E} \Delta\eta + \frac{\partial C_{H_E}}{\partial\xi} \Delta\xi \right) +$$

$$+ r_E m_E g \Delta n - (x_E r_E m_E + I_E \cos\lambda) \Delta\dot{q} -$$

$$- I_E \sec\lambda \Delta\ddot{\eta} - (y_E r_E m_E - I_E \sin\lambda) \Delta\dot{p}. \tag{A.4}$$

A similar expression may be written for the starboard aileron incremental jack moment.

$$-\Delta H_K = \tfrac{1}{2}\rho_0 V_i^2 S_A c_A \left(b_{1_A} \Delta\alpha + b_{2_A} \Delta\xi + \frac{\partial C_{H_A}}{\partial\eta} \Delta\eta \right) +$$

$$+ r_A m_A g \Delta n - (x_A r_A m_A + I_A \cos\lambda) \Delta\dot{q} -$$

$$- I_A \sec\lambda \Delta\xi - (y_A r_A m_A - I_A \sin\lambda) \Delta\dot{p}. \tag{A.5}$$

APPENDIX B

Evaluation of b_2 and Cross-control Derivatives from Control Pulses.

If a control pulse is of short duration, at the instant of maximum control application the aircraft will not have responded sufficiently to affect significantly the aerodynamic hinge moments. Consequently at that instant, incremental values measured from the initial trim condition, $\Delta\alpha$, Δp and Δq are negligible, but in the present tests their time derivatives are significant.

In the elevator pulses analysed no significant aileron movement occurred, and consequently $\Delta\dot{p}$ was zero. The incremental values of the elevator and aileron jack moments, for both the port and starboard sides are given by:

$$-\Delta H_J = \tfrac{1}{2}\rho_0 V_i^2 S_E c_E b_{2_E} \Delta\eta + r_E m_E g \Delta n - (x_E r_E m_E + I_E \cos\lambda)\Delta\dot{q} - I_E \sec\lambda\,\Delta\ddot{\eta} \tag{B.1}$$

$$-\Delta H_K = \tfrac{1}{2}\rho_0 V_i^2 S_A c_A \frac{\partial C_{H_A}}{\partial\eta}\Delta\eta + r_A m_A g\ \Delta n - (x_A r_A m_A + I_A \cos\lambda)\Delta\dot{q}. \tag{B.2}$$

These equations can be solved for b_{2_E} and $\partial C_{H_A}/\partial\eta$, the remaining terms being either known aircraft parameters or variables of motion. In fact, only $\Delta\eta$ was measured, $\Delta\ddot{\eta}$ and $\Delta\dot{q}$ were not measured and Δn was measured by an instrument too coarse to give the required resolution. As we are dealing here with the initial response to a control pulse before rate of pitch and incidence have had time to build up to any extent, the effects of aircraft damping may be ignored, giving:

$$\Delta\dot{q} = \frac{2g}{C_L i_B \bar{c}}\,\frac{\partial C_m}{\partial\eta}\Delta\eta \tag{B.3}$$

$$\Delta n = \frac{\partial C_L}{\partial\eta}\,\frac{\Delta\eta}{C_L}. \tag{B.4}$$

Values of $\partial C_m/\partial\eta$ and $\partial C_L/\partial\eta$ have been obtained from earlier tests made on the aircraft and reported in Ref. 5.

The most plausible procedure for estimating the value of $\Delta\ddot{\eta}$ is to assume that the elevator movement can be approximated to a sine wave in this region, say

$$\Delta\eta(t) = \Delta\eta^{\,\max}\sin\left(\Pi\frac{t}{T}\right) \tag{B.5}$$

where T is the duration of the control pulse.

The value coinciding with the maximum η is,

$$\Delta\ddot{\eta} = -\Delta\eta\left(\frac{\Pi}{T}\right)^2. \tag{B.6}$$

Having thus conveniently defined all the variables in terms of $\Delta\eta$, the peak value of elevator, equations (B.1) and (B.2) can now be solved for b_{2_E} and $\partial C_{H_A}/\partial\eta$ for both port and starboard controls

$$b_{2_E} = \frac{-\Delta H_J}{\tfrac{1}{2}\rho_0 V_i^2 S_E c_E \Delta\eta} - \frac{S}{S_E c_E}\left[\frac{r_E m_E}{m}\frac{\partial C_L}{\partial\eta} - \frac{2(x_E r_E m_E + I_E \cos\lambda)}{m\, i_B\, \bar{c}}\frac{\partial C_m}{\partial\eta}\right.$$

$$\left. + \frac{I_E \sec\lambda}{\tfrac{1}{2}\rho_0 V_i^2 S}\left(\frac{\Pi}{T}\right)^2\right] \tag{B.7}$$

13

$$\frac{\partial C_{H_A}}{\partial \eta} = \frac{-\Delta H_k}{\frac{1}{2}\rho_0 V_i^2 S_A c_A \Delta \eta} - \frac{S}{S_A c_A}\left[\frac{r_A m_A}{m}\frac{\partial C_L}{\partial \eta} - \frac{2(x_A r_A m_A + I_A \cos \lambda)}{m i_B \bar{c}}\frac{\partial C_m}{\partial \eta}\right].$$ (B.8)

Considering the aileron pulse, the acceleration in roll is determined as for $\dot{q}$ in equation (B.3).

$$\dot{p} = \frac{2g}{C_L i_A s} l_\xi \Delta \xi.$$ (B.9)

Flight[8] and tunnel[9,10] values of l_ξ show reasonable agreement, and where possible flight values have been used. Applying a procedure identical to the elevator case, equations for the evaluation of b_{2_A} and the cross derivative $\partial C_{H_E}/\partial \xi$ can then be obtained, giving

$$b_{2_A} = \frac{-\Delta H_k}{\frac{1}{2}\rho_0 V_i^2 S_A c_A \Delta \xi} - \frac{S}{S_A c_A}\left[\frac{I_A \sec \lambda}{\frac{1}{2}\rho_0 V_i^2 S}\left(\frac{\Pi}{T}\right)^2 \mp \frac{2(y_A r_A m_A - I_A \sin \lambda)}{m i_A s} l_\xi\right]$$ (B.10)

$$\frac{\partial C_{H_E}}{\partial \xi} = \frac{-\Delta H_l}{\frac{1}{2}\rho_0 V_i^2 S_E c_E \Delta \xi} - b_{2_E}\frac{\Delta \eta}{\Delta \xi} \pm \frac{S}{S_E c_E}\frac{2(y_E r_E m_E - I_E \sin \lambda)}{m i_A s} l_\xi$$ (B.10)

where the alternate signs apply to starboard and port respectively. In the present tests, a small correction for $\Delta \eta$ has been retained in equation (B.11) as this term is significant, although $\Delta \ddot{\eta}$ is negligible.

APPENDIX C

Determination of b_1 from the Stick Fixed Longitudinal Short Period Oscillations.

For this motion incremental values are measured between successive peaks of the aircraft oscillation. In the present tests, Δp, $\Delta \dot{p}$, $\Delta \dot{\eta}$ and $\Delta \dot{\xi}$ are negligible. Following similar reasoning to that of Appendix B, it can be shown from Ref. 11 that the aircraft motions in normal acceleration and pitching are given by,

$$\Delta n = \frac{a \, \Delta \alpha}{C_L} \tag{C.1}$$

$$\Delta \dot{q} = -\mathscr{I} \left(\frac{\bar{q}}{\bar{n}} \right) \frac{a}{C_L} \Delta \alpha . \tag{C.2}$$

This relation has been derived ignoring the effect of the damping derivatives, since the damping was small in the flight tests. $\mathscr{I}$ is the frequency of the longitudinal short period oscillation and $(\bar{q}/\bar{n})$ is the amplitude ratio of pitching velocity to normal acceleration in this oscillation. Both these parameters, and the un-trimmed lift curve slope, were measured in previous flight tests[12].

The incremental jack moment for the elevator is, from equation (A.4),

$$-\Delta H_J = \tfrac{1}{2} \rho_0 V_i^2 S_E c_E \left(b_{1_E} \Delta \alpha + b_{2_E} \Delta \eta + \frac{\partial C_{H_E}}{\partial \xi} \Delta \xi \right)$$

$$+ \left[r_E m_E g + (x_E r_E m_E + I_E \cos \lambda) \mathscr{I} \left(\frac{\bar{q}}{\bar{n}} \right) \right] \frac{a}{C_L} \Delta \alpha . \tag{C.3}$$

From this equation b_{1_E} may be derived, as b_{2_E} and $\partial C_{H_E}/\partial \xi$ are known from Appendix B. In the present tests, the term involving $\Delta \xi$ is negligible. Thus

$$b_{1_E} = \frac{-\Delta H_J}{\tfrac{1}{2} \rho_0 V_i^2 S_E c_E \Delta \alpha} - b_{2_E} \frac{\Delta \eta}{\Delta \alpha} - \frac{aS}{S_E c_E} \left[\frac{r_E m_E}{m} + (x_E r_E m_E + I_E \cos \lambda) \frac{\mathscr{I}}{mg} \left(\frac{\bar{q}}{\bar{n}} \right) \right] . \tag{C.4}$$

In the case of the aileron, the terms in both $\Delta \eta$ and $\Delta \xi$ are negligible in the present tests. Thus,

$$b_{1A} = \frac{-\Delta H_k}{\tfrac{1}{2} \rho_0 V_i^2 S_A c_A \Delta \alpha} - \frac{aS}{S_A c_A} \left[\frac{r_A m_A}{m} + (x_A r_A m_A + I_A \cos \lambda) \frac{\mathscr{I}}{mg} \left(\frac{\bar{q}}{\bar{n}} \right) \right] . \tag{C.5}$$

15

Evaluation of Elevator and Aileron Hinge Moment Derivatives due to incidence, b_1, from flight at different values of normal acceleration.

In flight at constant normal acceleration, the angular acceleration terms can be ignored and equations (A.1) and (A.2) reduce to,

$$-H_J = \tfrac{1}{2}\rho_0 V_i^2 S_E c_E \left[b_{0_E} + b_{1_E}\alpha + b_{2_E}\eta + \frac{\partial C_{H_E}}{\partial \xi} \right] + r_E m_E gn \qquad (D.1)$$

a similar equation may be written for the ailerons.

Taking tests at the same Mach number, but different normal accelerations, say, n_1 and n_2, we get,

$$b_{1_E} = \frac{-1}{\tfrac{1}{2}\rho_0 S_E c_E \Delta\alpha} \left[\frac{(H_{J_2}+r_E m_E g\, n_2)}{V_{i\,2}^2} - \frac{(H_{J_1}+r_E m_E g\, n_1)}{V_{i\,1}^2} \right] - b_{2_E}\frac{\Delta\eta}{\Delta\alpha} - \left[\frac{\partial C_{H_E}}{\partial \xi}\right]\frac{\Delta\xi}{\Delta\alpha} \qquad (D.2)$$

where suffices 1 and 2 refer to the different test conditions and Δ signifies the increment between test conditions. b_{2_E} and $\partial C_{H_E}/\partial \xi$ have been derived in Appendix B.

A similar expression can be derived for the ailerons.

TABLE 1

Leading Aircraft Dimensions.

Gross wing area	$S = 360\ \text{ft}^2$
Semi-span	$s = 13\cdot42\ \text{ft}$
Nominal centreline chord	$25\ \text{ft}$
Tip chord	$1\cdot83\ \text{ft}$
Mean aerodynamic chord	$\bar{c} = 16\cdot75\ \text{ft}$
Wing section	4% Symmetrical, max t/c at $29\cdot5\%$ chord
Trailing-edge angle	$5\cdot2°$
Leading-edge sweepback	$59\cdot9°$
Trailing-edge sweepback	0
Twist	0
Dihedral	0
Incidence with respect to fuselage datum	$+1\cdot5°$
Mean weight at test condition	$12800\ \text{lb}$
Pitching moment of inertia coefficient, i_B	$0\cdot269$
Rolling moment of inertia coefficient, i_A	$0\cdot0558$

TABLE 2

Control Surface Details.

Aileron

m_A, mass	2·38 slugs
I_A, moment of inertia about the hinge	2·77 slugs ft²
S_A, area aft of hinge	16·04 ft²
c_A, mean chord aft of hinge	2·70 ft
r_A ⎫	0·65 ft
x_A ⎬ Fig. 15	8·52 ft
y_A ⎭	10·01 ft
λ, sweep of hinge	9·7°
Horn-balance area	0·57 ft²
Rigged up angle	3°

Elevator

m_E, mass	3·15 slugs
I_E, moment of inertia about the hinge	6·17 slugs ft²
S_E, area aft of hinge	20·18 ft²
c_E, mean chord aft of hinge	3·69 ft
r_E ⎫	0·75 ft
x_E ⎬ Fig. 15	7·57 ft
y_E ⎭	4·53 ft
λ, sweep of hinge	9·7°
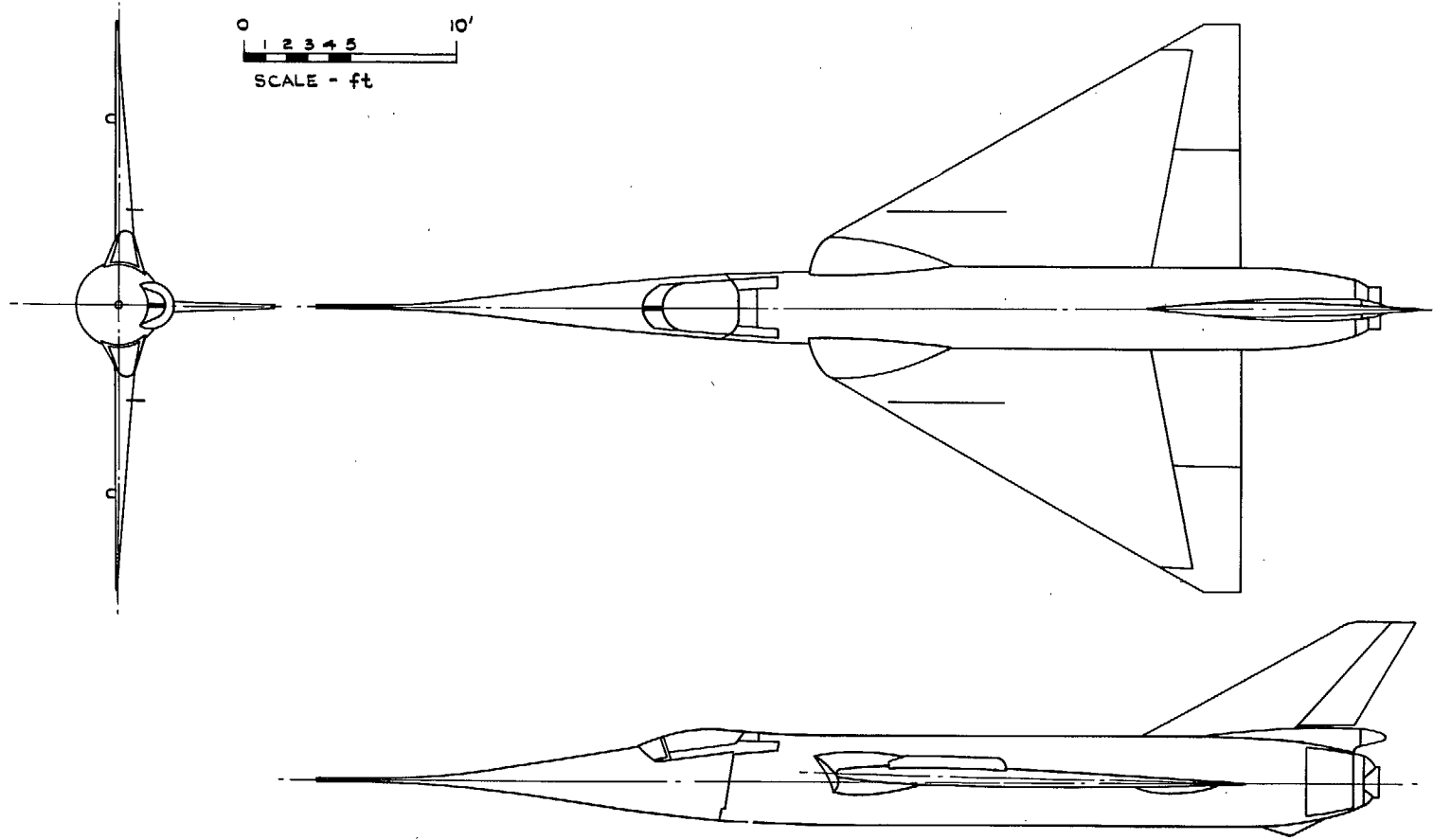
FIG. 1. General arrangement of the Fairey Delta 2.

FIG. 2.   The Fairey Delta 2.
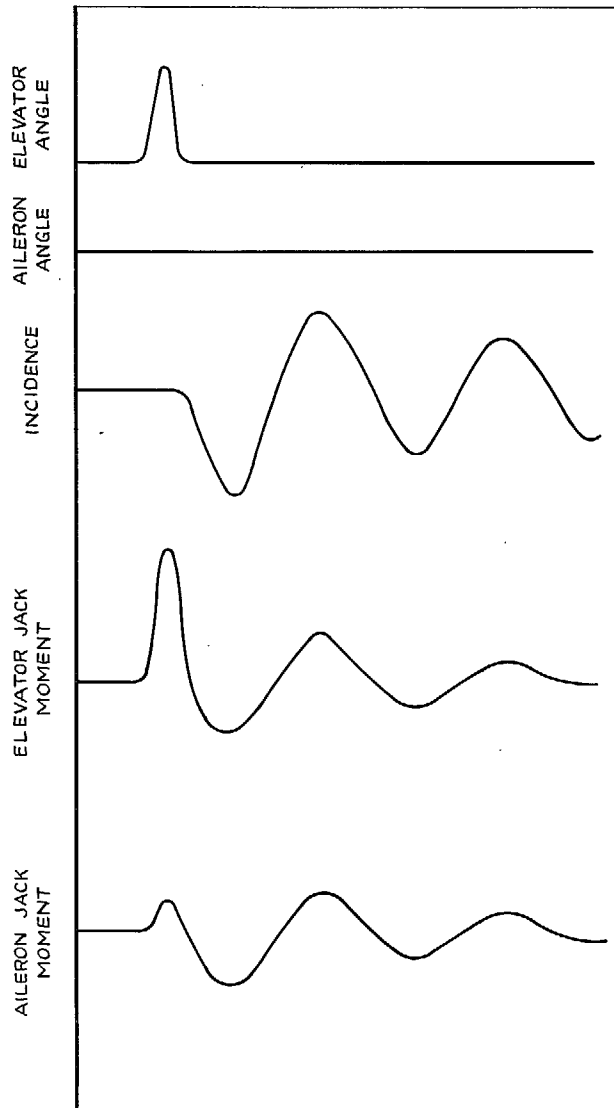
FIG. 3a. Idealised time history of an elevator pulse.
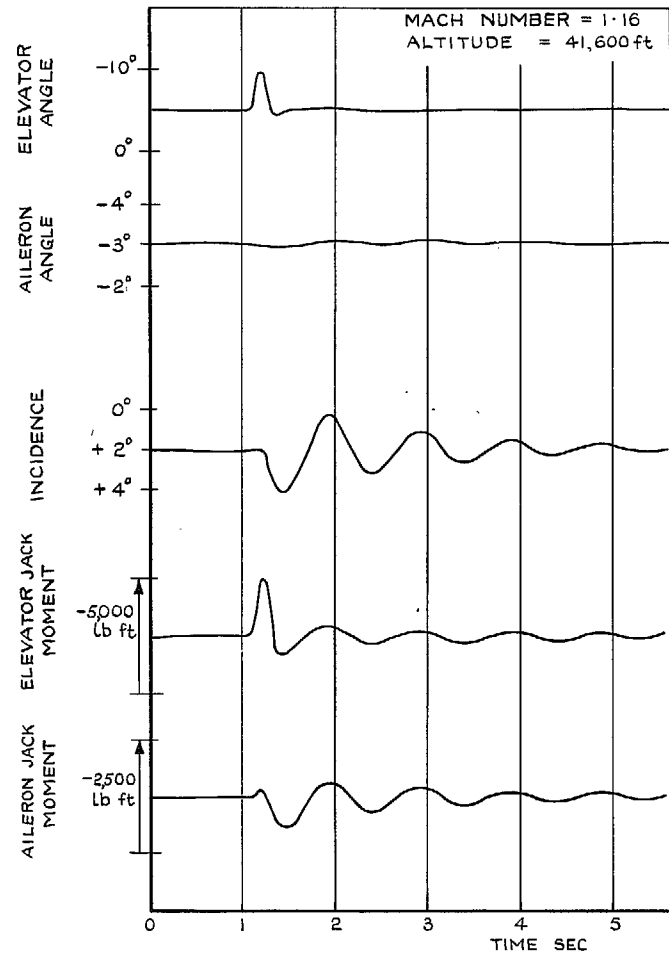
FIG. 3b. Flight record of an elevator pulse.
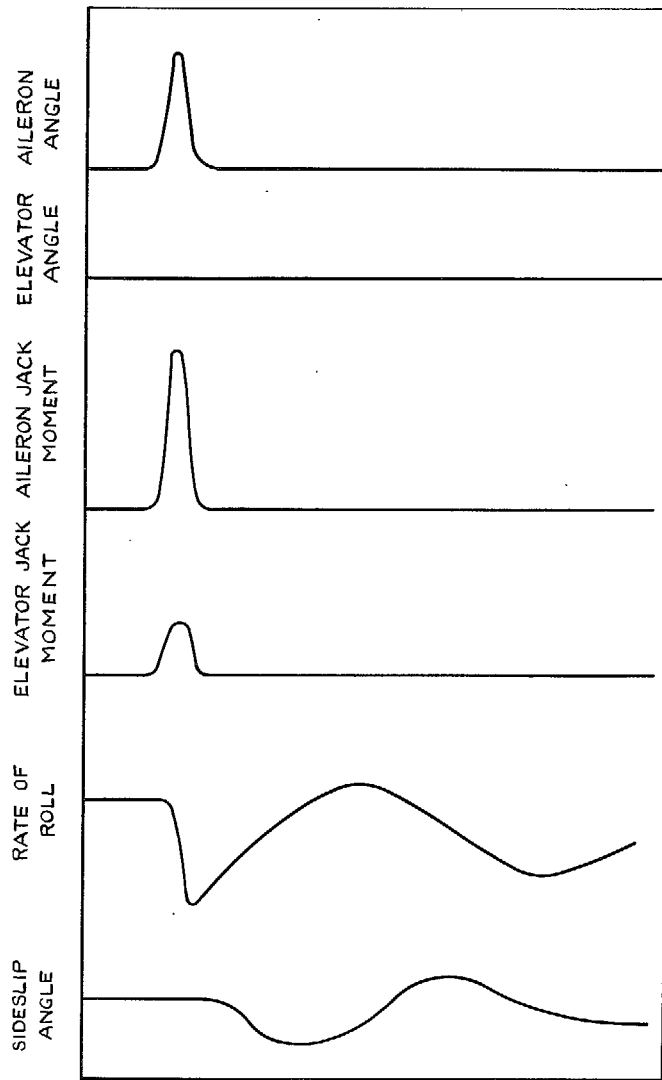
FIG. 4a. Idealised time history of an aileron pulse.
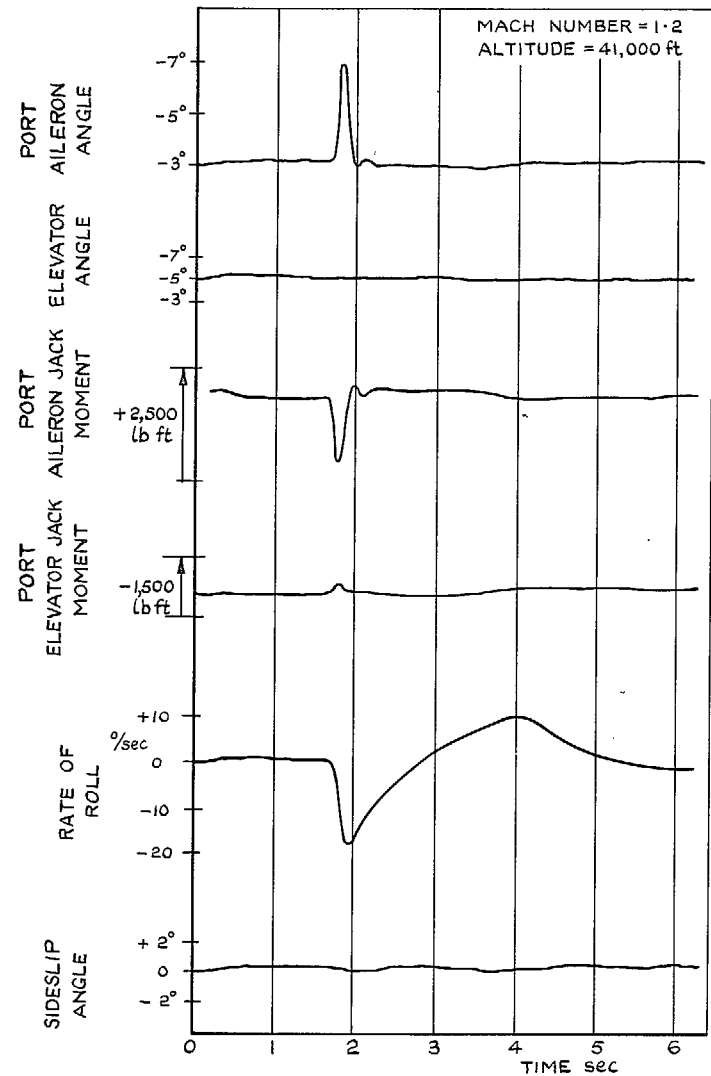
FIG. 4b. Flight record of an aileron pulse.
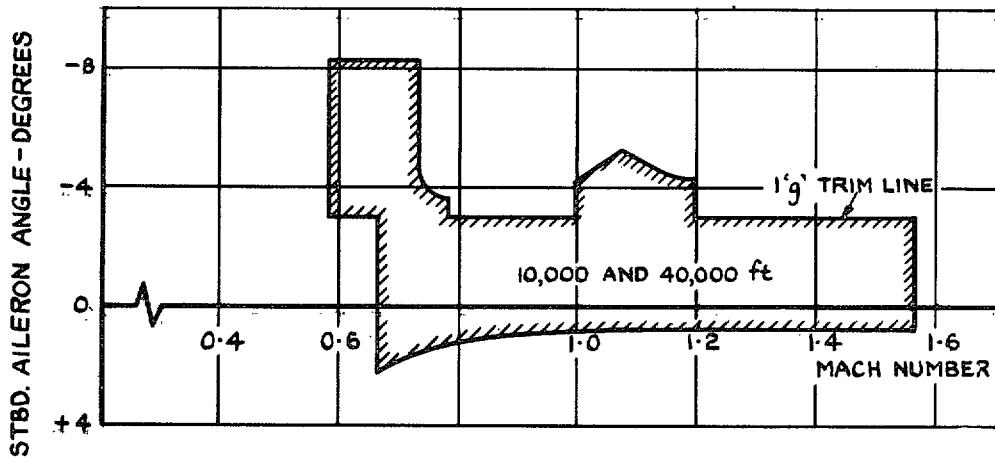
FIG. 5. Envelope of aileron angles covered in the flight tests.
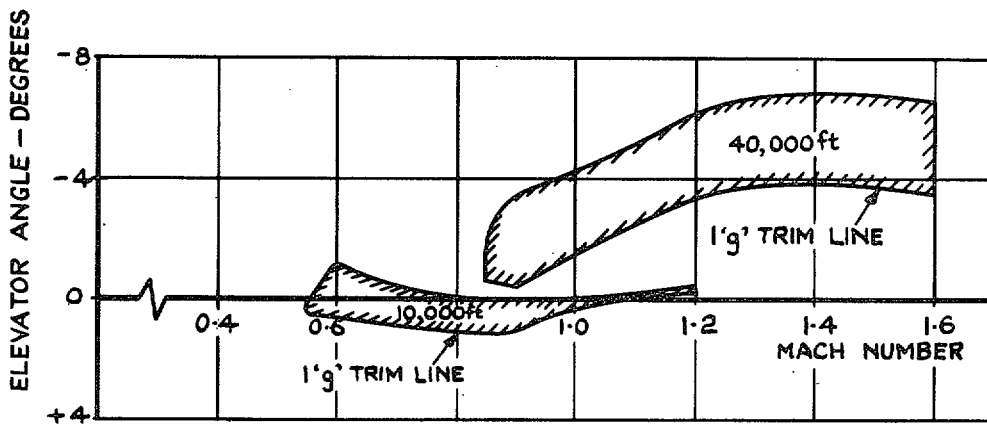
FIG. 6. Envelope of elevator angles covered in the flight tests.
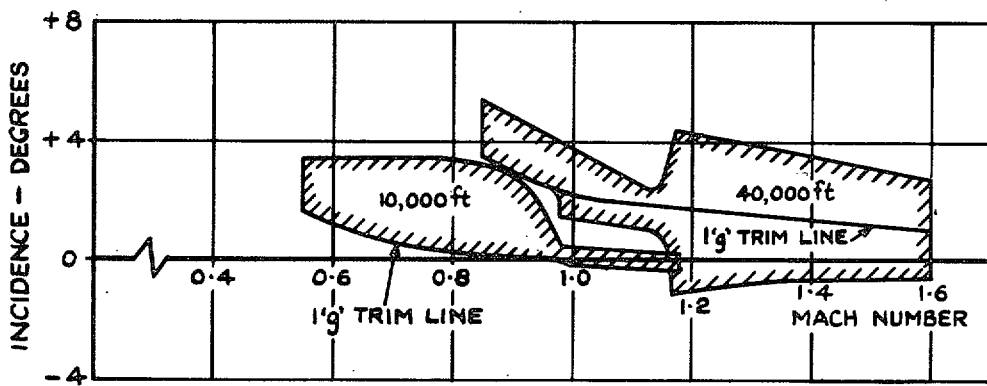
FIG. 7. Envelope of incidence covered in the flight tests.
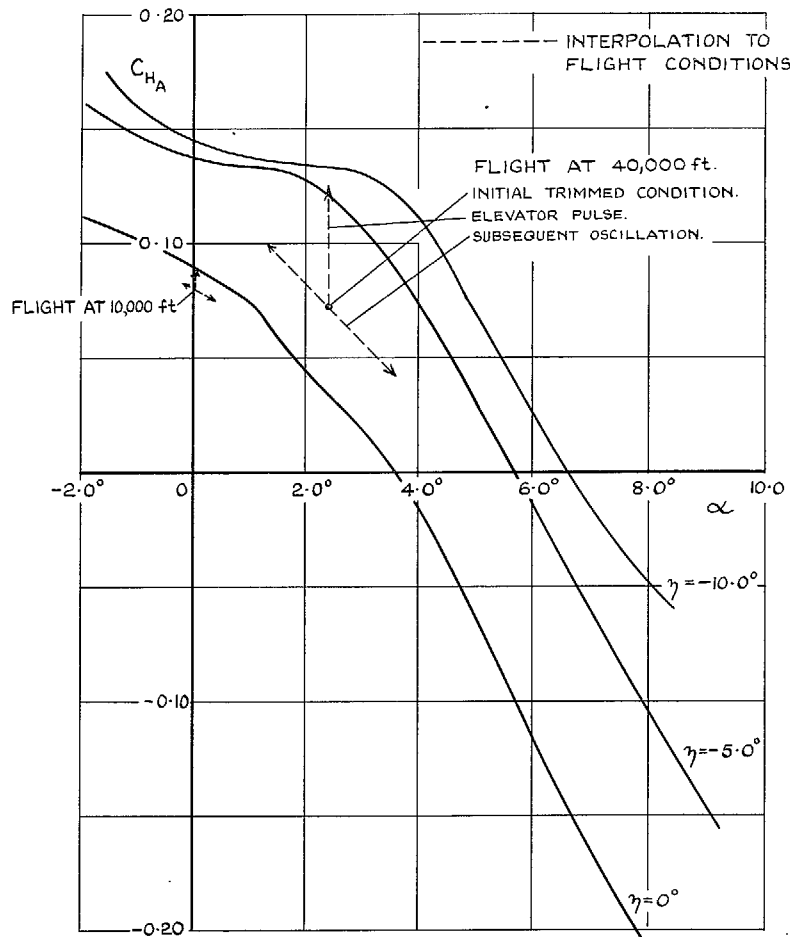
FIG. 8.   A.R.A. wind-tunnel results at $M = 1.02$
for aileron hinge moments.
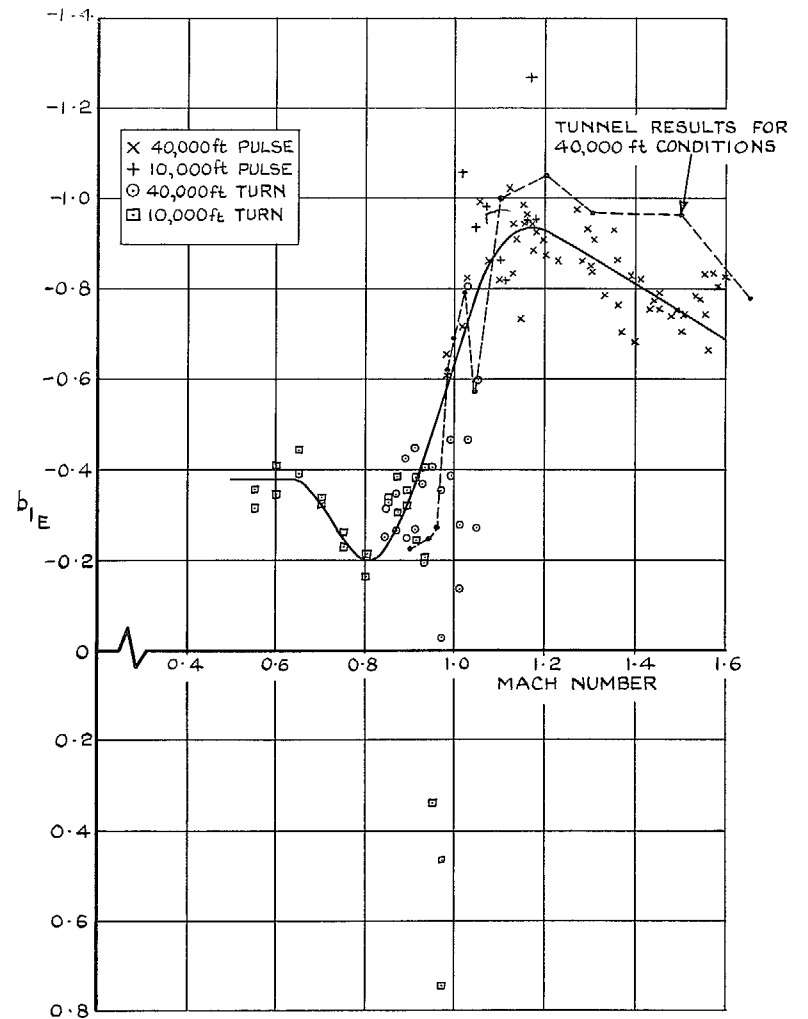
FIG. 9.   Elevator hinge moment due to incidence
derivative *versus* Mach number.
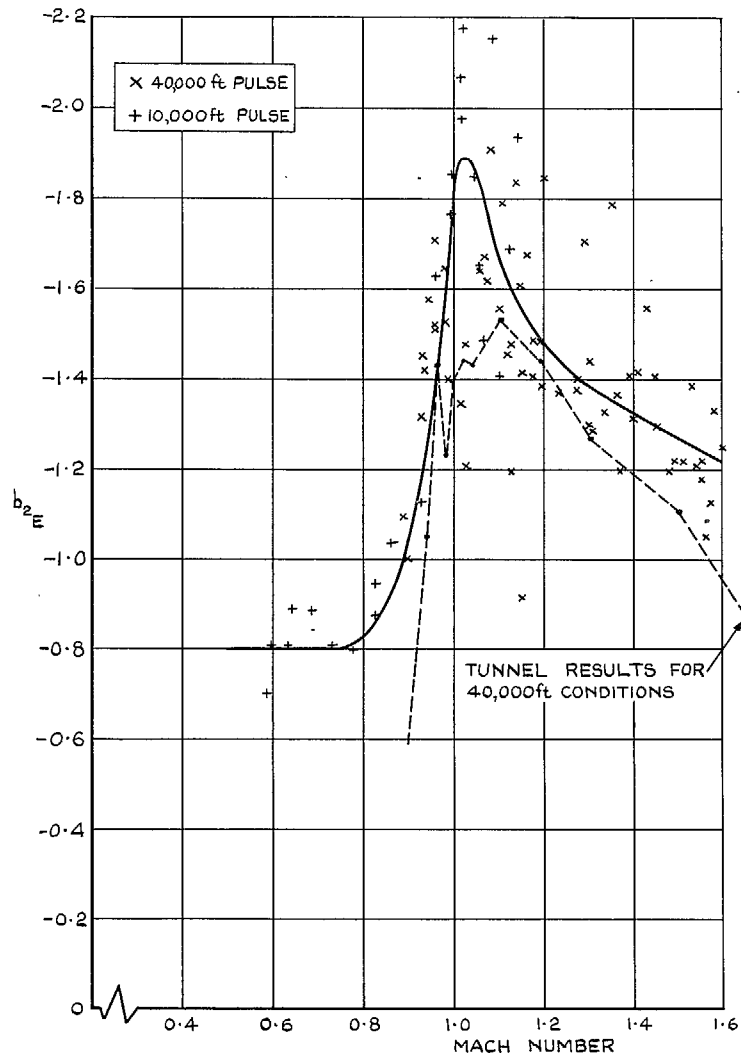
FIG. 10. Elevator hinge moment due to elevator-angle derivative *versus* Mach number.
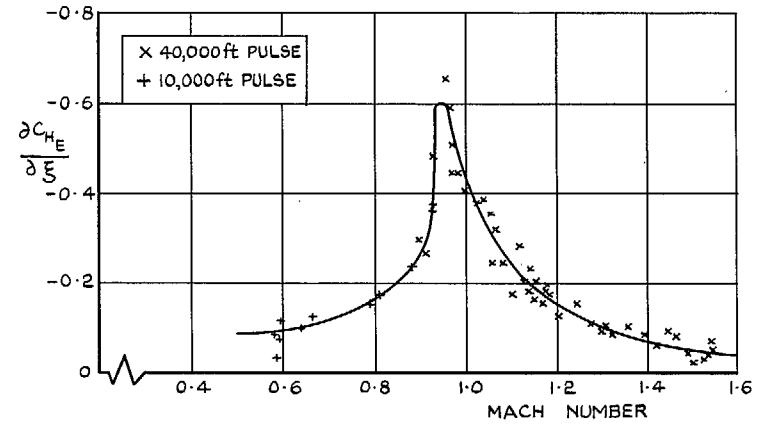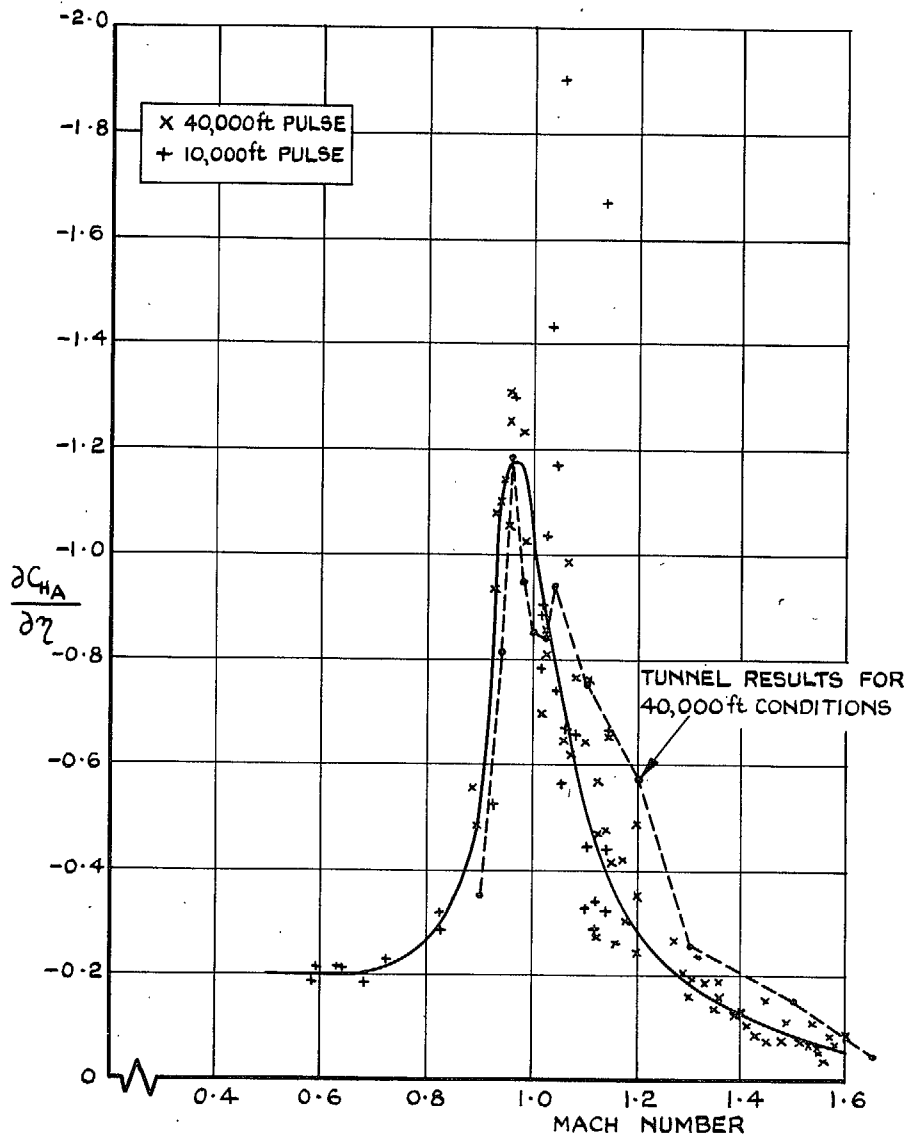

FIG. 11. Elevator hinge moment due to aileron-angle derivative versus Mach number.
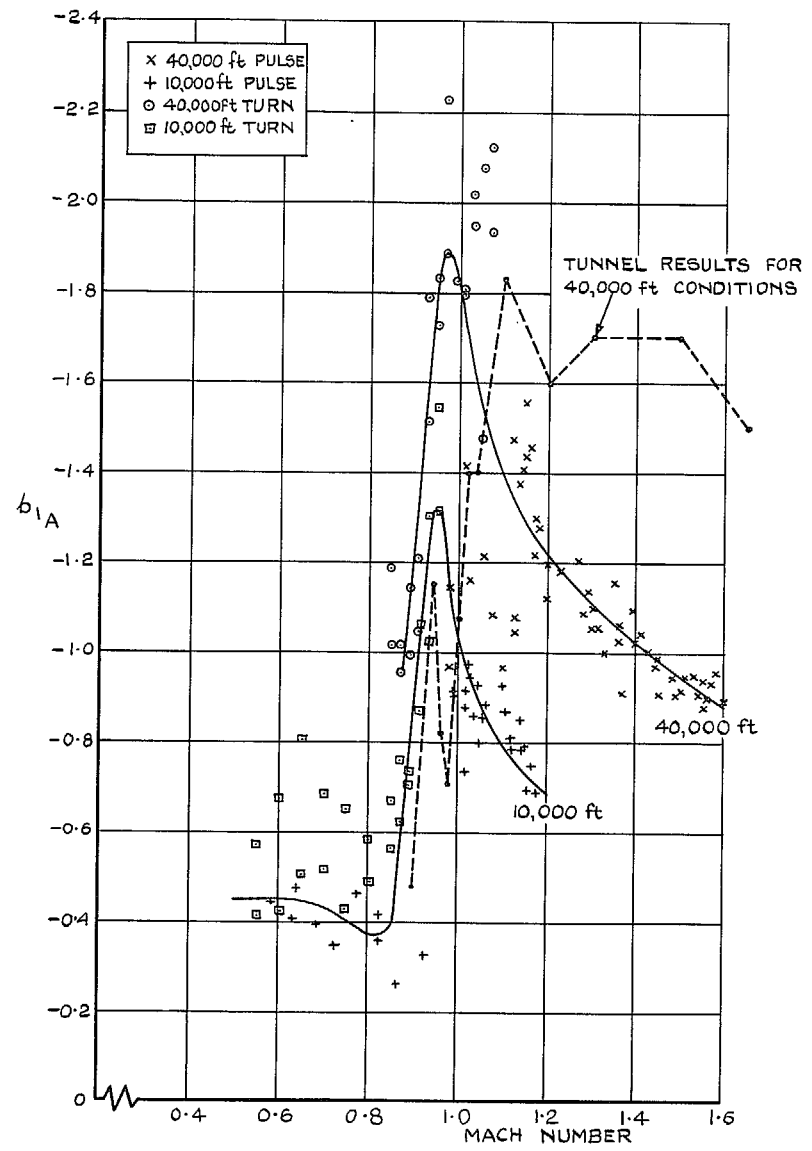
FIG. 12. Aileron hinge moment due to incidence
Derivative *versus* Mach number.
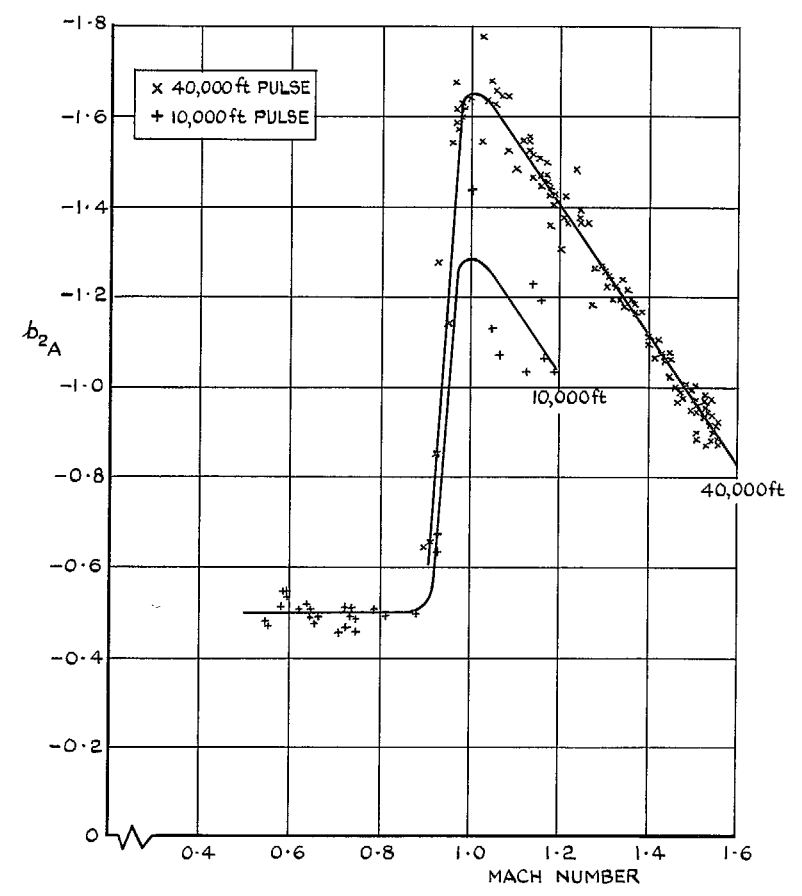
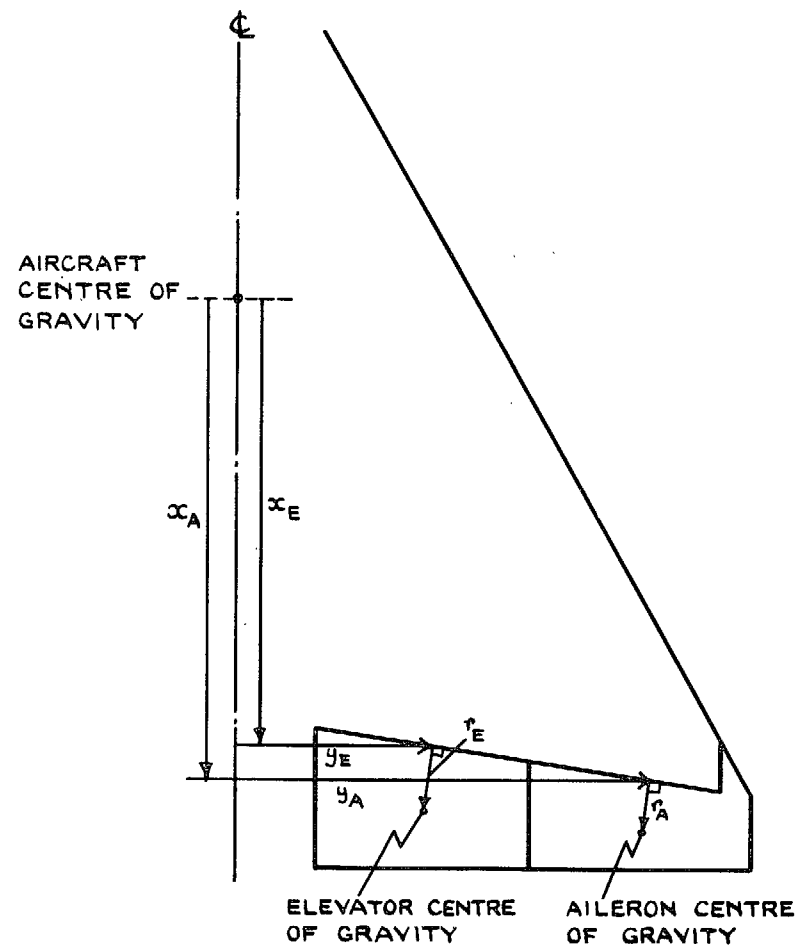FIG. 13. Aileron hinge moment due to aileron-
angle derivative *versus* Mach number.

Printed in Wales for Her Majesty's Stationery Office by Allens Printers (Wales) Limited.

Dd.129527   K5

FIG. 14.   Aileron hinge moment due to elevator-
angle derivative *versus* Mach number.

FIG. 15.   Control geometric data.